Computers & Operations Research 44 (2014) 1–12

Contents lists available at ScienceDirect

Computers & Operations Research

journal homepage: www.elsevier.com/locate/caor

# A conflict–congestion model for pedestrian–vehicle mixed evacuation based on discrete particle swarm optimization algorithm

Xinlu Zong [a,*], Shengwu Xiong [b], Zhixiang Fang [c,*]

[a] School of Computer Science and Technology, Hubei University of Technology, Wuhan 430068, China
[b] School of Computer Science and Technology, Wuhan University of Technology, Wuhan 430070, China
[c] State Key Laboratory for Information Engineering in Surveying, Mapping and Remote Sensing, Wuhan University, 129 Luoyu Road, Wuhan 430079, China

ARTICLE INFO

Available online 31 October 2013

*Keywords:*
Simulation
Pedestrian–vehicle mixed evacuation
Discrete particle swarm optimization algorithm
Temporal–spatial conflict
Temporal–spatial congestion

ABSTRACT

A simulation model based on temporal–spatial conflict and congestion for pedestrian–vehicle mixed evacuation has been investigated. Assuming certain spatial behaviors of individuals during emergency evacuation, a discrete particle swarm optimization with neighborhood learning factor algorithm has been proposed to solve this problem. The proposed algorithm introduces a neighborhood learning factor to simulate the sub-group phenomenon among evacuees and to accelerate the evacuation process. The approach proposed here is compared with methods from the literatures, and simulation results indicate that the proposed algorithm achieves better evacuation efficiency while maintaining lower pedestrian–vehicle conflict levels.



## 1. Introduction

Pedestrian–vehicle mixed evacuation is an important and urgent issue which is confronted frequently by modern transportation, earth observation, geography, artificial intelligence, computer science, modern communications, and public health and security. In some types of large public areas, a huge number of pedestrians and vehicles are highly crowded together. Once catastrophic events such as hurricanes, fire, or terrorist attacks occur, pedestrians and vehicles crowd and congest together, which may lead to serious results for human beings. Recently, modeling and simulation of emergency evacuation have been attracting widespread attention from researchers [1,2].

However, the existing evacuation studies do not address the demands of mixed evacuation of pedestrians and vehicles. Currently, most evacuation models have focused on pedestrian evacuation from inside buildings [3] or vehicle evacuation over road networks [4]. Research on mixed evacuation of pedestrians and vehicles [5,6] is a more changeable and open issue in emergency management, particularly in the areas which integrate both building and roads.

On the other hand, only a few researches on evacuation modeling have been studied by using optimization algorithms. Existing optimization models involve optimizing only one objective for a single transportation mode or converting multiple objectives into a single-objective optimization problem for which the single optimal solution cannot offer decision support on multiple objectives.

The main difficulty in modeling and simulating pedestrian–vehicle mixed evacuation lies in the simulation of evacuation movements and the interaction behavior between pedestrians and vehicles. In this paper, pedestrian–vehicle temporal–spatial conflict and temporal–spatial congestion are defined. An evacuation model for mixed traffic flow based on temporal–spatial conflict and congestion is presented. In addition, a novel discrete particle swarm optimization with neighborhood learning factor (DPSONLF) algorithm is proposed to solve this mixed evacuation problem.

This paper is organized as follows. Section 2 discusses previous work related to simulation and modeling for evacuation. Section 3 presents a mixed evacuation model based on temporal–spatial conflict and temporal–spatial congestion. Section 4 introduces a DPSONLF algorithm based on discrete particle swarm optimization (DPSO) to simulate and optimize the evacuation process with mixed traffic flow. Section 5 analyzes and compares the simulation results using different optimization approaches. Finally, Section 6 draws conclusions and discusses directions for future research.

## 2. Related work

Current studies on mixed traffic flow usually focus on simulation [7,8]. Meng et al. [9] proposed a single-lane cellular automaton model to simulate mixed traffic with motorcycles. In the model, density-flow relations and the "lane-changing" behavior of motorcycles were investigated to find the relationship between the maximum flow

* Corresponding authors. Tel.: +86 13476068149.
*E-mail addresses:* zongxinlu@126.com (X. Zong), zxfang@whu.edu.cn (Z. Fang).

0305-0548/$ - see front matter © 2013 Elsevier Ltd. All rights reserved.
http://dx.doi.org/10.1016/j.cor.2013.10.015

and motorcycle density. Si et al. [5] presented link resistance functions based on travel demand for different roads in an urban mixed traffic network and analyzed the characteristics of different traffic modes including cars, buses, and bicycles. Xie et al. [6] proposed a two-dimensional car-following model to depict the features of mixed traffic flow consisting of motorized and non-motorized vehicles. Characteristics of mixed traffic flow were studied by investigating the interaction between left-turning non-motorized vehicle flow and straight-ahead motorized vehicle flow at a typical unsignalized intersection. However, the researchers modeled mixed traffic flow under normal conditions, which is somewhat inappropriate for emergency situations. As for evacuation modeling, some studies have been done for the problem inside buildings [10] or in road networks [11]. For example, Chen et al. [12] presented a force-driving cellular automaton model considering the social forces on cell movement, such as the desire of a pedestrian to exit, the repulsive interaction among or between pedestrians, and the effect of obstacles, to investigate the evacuation behaviors of pedestrians at a T-shaped intersection. The model studied the pedestrian evacuation problem from the microscopic point of view, but neglected attraction forces to simulate the conformity phenomenon. Guo et al. [13] investigated the route choice in pedestrian evacuation under conditions of both good and zero visibilities. They presented a microscopic evacuation model with discrete space representation to simulate the behavior of pedestrians. As for vehicle evacuation, Tanaka et al. [14] studied the mixing of vehicles on a two-lane highway in hurricane evacuation and proposed a deterministic model of two-lane traffic in which vehicles changed lanes using a deterministic rule. Bretschneider and Kimms [15] proposed a two-stage heuristic solution approach for a pattern-based mixed integer dynamic network flow model that restructured the traffic routing for the case of an evacuation. In their model, the time-expanded network and a relaxation-based heuristic were used to minimize the evacuation-time while prohibiting conflicts within intersections.

These models for either pedestrian or vehicle evacuation mainly focused on the microscopic evacuation behavior of pedestrians or vehicles. But the real evacuation scenarios usually involves the area integrated both building and roads around. Therefore, pedestrians inside a building and vehicles on the roads around need to be considered as evacuees simultaneously. And the interaction among and between pedestrians and vehicles during evacuation process should be analyzed. Recently, some researchers studied modeling and simulation of mixed evacuation problem. For example, Jin et al. [16] developed a mixed traffic evacuation model to study the influence of different transport modes. These simulations focused on the evacuation time for various combinations of people, bicycles, and motor vehicles. Zong et al. [17] studied the mixed evacuation problem and proposed model considering the factors such as congestion and the interaction between pedestrians and vehicles, but the model has not taken the potential conflict between pedestrians and vehicles into account, which is crucial to evacuation efficiency.

Currently, multi-objective optimization algorithms and swarm intelligence have been used to simulate and solve evacuation problems for making evacuation plans which satisfy more than one objective [18–20]. A number of optimization algorithms or techniques, including the ant colony optimization algorithm [21,22], the particle swarm optimization algorithm [23,24], game theory [25], agent theory [26,27], non-dominated sorting genetic algorithm [28], and genetic algorithm [29] in general, have been used to solve evacuation problems. For example, Izquierdo et al. [23] used particle swarm optimization to simulate and forecast evacuation time. The model took minimizing distance from an exit as the optimization objective. Zheng et al. [24] also presented a PSO-based heterogeneous evacuation model. In the model, the distance from a particle to the nearest exit was taken as the fitness function and the pedestrian's velocity was impacted by the local pedestrian's density. The model simulated the pedestrian's psychology of rapid evacuation and investigated the relationship between velocity and density, but the tendency of going with the crowd was not considered. Xie et al. [30] proposed a method to solve a lane-based evacuation network optimization problem. The objective of the approach was to minimize the number of crossing points at the given intersection and an integrated Lagrangian relaxation and tabu search solution method were developed. Most of these evacuation models considered one aspect as optimization objective. However, several factors need to be taken into account simultaneously, especially for such complex optimization problems, to make effective evacuation plans.

Stepanov and Smith [31] generated an evacuation plan with objectives including minimization of total clearance time, minimization of total distance traveled, and the avoidance of blocking. Saadatseresht et al. [28] used multi-objective evolutionary algorithms and a geographical information system for evacuation planning. In their model, maximizing the capacity of safe areas and minimizing distance were defined as two optimization objectives, and the NSGA-II algorithm was used to determine the distribution of evacuees into safe areas in a GIS environment. Tzeng et al. [32] constructed a multi-objective model for delivering commodities to demand points in an emergency situation using fuzzy multi-objective programming. Lim et al. [33] presented a capacity constrained network flow optimization approach for finding shortest evacuation paths with maximum evacuees. Dijkstra's algorithm was used to find the evacuation paths first and then a greedy algorithm for finding the maximum flow of each path. These evacuation models optimized more than one objective in evacuation process. But the interaction between evacuees and the congestion level at each time interval were not studied. And most of these multi-objective models converted several objectives into a single objective. Few studies have optimized the evacuation process considering multiple objectives simultaneously, especially both in temporal and spatial aspects.

Recently, Fang et al. [34] proposed and demonstrated a space–time use efficiency model on the basis of trajectories in the case of mixed vehicle and pedestrian flows in intersections. A two-tier hybrid multi-objective optimization algorithm was presented to plan vehicle and pedestrian turning movement directions, and three objectives: average evacuation time, the overall length traveled, and space–time use efficiency of network were optimized. But the space–time objectives of conflict and congestion caused by the interaction between pedestrians and vehicles were not considered.

From a review of evacuation models, two challenges are evident. The first challenge is modeling the evacuation process not only for a single traffic mode, but also for pedestrians and vehicles mixed together. The second challenge is solving the mixed evacuation problem using multi-objective optimization algorithms.

In this research, the evacuation problem with mixed traffic flow has been solved with the help of a new temporal–spatial evacuation model using a new discrete particle swarm optimization approach with a neighborhood learning factor algorithm. Different optimization methods available in the literatures are also evaluated and compared. The proposed approach may help the decision makers make temporal–spatial evacuation plans more rationally and develop feasible strategies.

## 3. Evacuation model based on temporal–spatial conflict and congestion

### 3.1. Mixed evacuation problem

Mixed pedestrian–vehicle evacuation as studied in this paper refers to the problem that in an emergency situation, people in public buildings, together with pedestrians and vehicles outside the buildings, need to be transferred out of an integrated environment with buildings and surrounding roads.

Generally, pedestrian behaviors, such as the possibility that pedestrians may not abide by the traffic laws and pedestrian group effects, mean that pedestrians are usually more "aggressive" than vehicles. For example, vehicles will decelerate voluntarily before stop lines to avoid conflicts with pedestrians, while pedestrians always cross streets as soon as possible when they feel the situation is safe. In an emergency situation, however, vehicles may not give way to pedestrians, but rather may compete for the right-of-way against pedestrians [35]. The main characteristics of evacuees include arching, clogging, and faster-is-slower behaviors [36], and the three forces of repulsion, friction, and attraction can be used to explain complex behaviors during an evacuation process. Collective panic phenomena may result in complex individual-level behaviors and interactions among individuals.

### 3.2. Evacuation network description

An evacuation network, generally represented by nodes and arcs, is a structure of regions accessible to individuals during an evacuation. In this paper, the study area includes a large building and the road network around the building. Therefore, roads, squares, and open spaces are accessible regions for pedestrians, while roads are accessible for vehicles. All the accessible regions are viewed as nodes, and the connections between accessible regions are represented as arcs. The evacuation network can then be stated as follows.

According to the connections between accessible regions, construct an emergency evacuation network, which is defined as a graph $G(N,A)$, where $N=\{1,2,...,n\}$ is the set of nodes and $A \subseteq N \times N$ is the set of arcs. The properties of a node include the capacity of the region, whether or not it allows vehicles access, and the state of the node. There are four kinds of state for a node: unoccupied, occupied by pedestrian, occupied by vehicle, and mixed with pedestrian and vehicle. At any time, a node is in one of these four states.

### 3.3. Individuals under evacuation

The individual under evacuation in a mixed traffic condition is either a pedestrian or a vehicle in this study. From the time before the emergency event happens to the time that all evacuees have reached safe areas, each individual is at one of the four states: normal state without any emergency event, evacuating state when the individual is under emergent situation, clogging state when congested with other individuals, and safe state when the individual reaches any exit. One state can be converted to another state under certain conditions, and the transformation rule of an individual is depicted in Fig. 1.

An individual pedestrian is allowed accessing all adjacent accessible regions; while vehicles are only allowed accessing roadways.

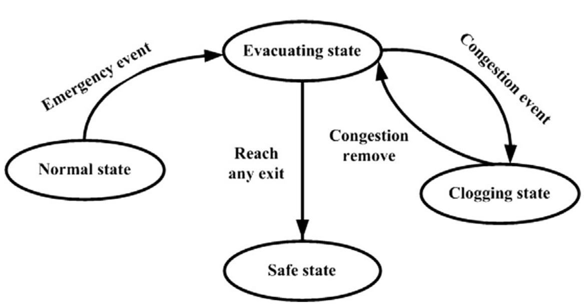


**Fig. 1.** State transition diagram of evacuee.

### 3.4. Temporal–spatial conflict

During the evacuation process, different individuals evacuate from their respective different initial positions to their final exits by various different intermediate routes. As a result, the movement tracks of individuals have different temporal and spatial distributions. As shown in Fig. 2, two evacuees passing from the same initial point A to the same exit have different temporal and spatial paths due to their different time sequences.

Traffic conflict is one of the most crucial issues in multi-mode transportation. A traffic conflict can be generally defined as a traffic situation involving two or more participants in traffic approaching each other in space and time, and in such a way that they pose a risk of causing a real collision if they do not change their direction or speed. Traffic conflicts can be categorized into three basic types: diverging, merging, and crossing conflicts [37]. Traffic conflicts in emergency situations, however, are characterized mainly by the behaviors of pedestrians and vehicles in panic, which in turn aggravates conflicts between pedestrians and vehicles.

Denote $P^i_{ped}(t)$ as the proportion of pedestrians to total individuals in node $i$ at time $i$; the pedestrian–vehicle conflict can be calculated as shown in Eq. (1). When the proportion of pedestrians to total individuals is greater than 0.8 [38], a pedestrian–vehicle conflict occurs because of the large quantity of pedestrians:

$$Conflict_i(t) = \begin{cases} 0 & P^i_{ped}(t) < 0.8 \\ 1 & P^i_{ped}(t) \geq 0.8 \end{cases} \tag{1}$$

Eq. (1) indicates that pedestrian–vehicle conflict depends on the number of pedestrians due to the arbitrariness of pedestrian's movement.

Let $T$ be the time for evacuating all evacuees. $T$ can be divided into several time intervals, and the numbers of pedestrians and vehicles passing through during time interval $\Delta t$ are counted for each node. According to the ratio of pedestrians to vehicles during $\Delta t$, the cumulative degree of pedestrian–vehicle conflict can be obtained as follows:

$$F_2 = \sum_{i \in N} \sum_{t=0}^{T} Conflict_i(t)\Delta t \tag{2}$$

### 3.5. Temporal–spatial congestion

Let $\sigma^i_{ped}(t)$ and $\sigma^i_{veh}(t)$ be the pedestrian saturation degree and the vehicle saturation degree of node $i$ at time $t$. These can be

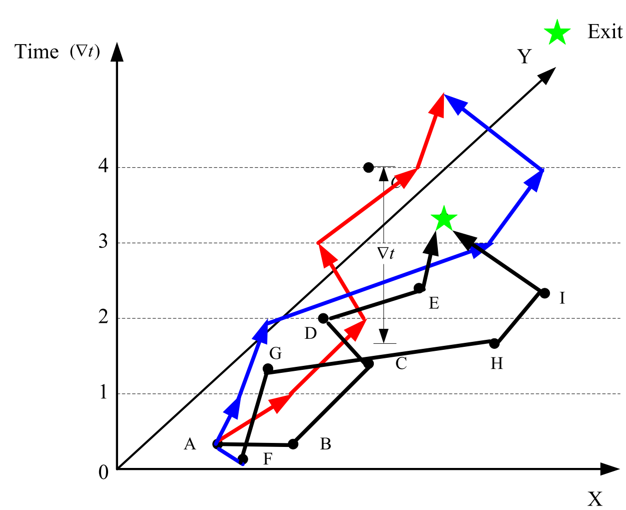


**Fig. 2.** Temporal and spatial paths of different individuals.

calculated by the following equations:

$$\sigma^i_{ped}(t) = \frac{N^i_{ped}(t)}{C^i_{ped}(t)} \tag{3}$$

$$\sigma^i_{veh}(t) = \frac{N^i_{veh}(t)}{C^i_{veh}(t)} \tag{4}$$

where $N^i_{ped}(t)$ ($N^i_{veh}(t)$) is the number of pedestrians (or vehicles) in node $i$ at time $t$ and $C^i_{ped}(t)$ ($C^i_{veh}(t)$) is the capacity of node $i$ for pedestrians (or vehicles).

In this paper, $Congestion^i_{ped}(t)$ and $Congestion^i_{veh}(t)$ are the congestion degrees of pedestrians and vehicles, respectively, in node $i$ at time $t$. The following functions are used to represent the relationship between congestion degree and saturation degree:

$$Congestion^i_{ped}(t) = \begin{cases} e^{r \cdot \sigma^i_{ped}(t)} & \text{if} \quad \sigma^i_{ped}(t) \geq 1 \\ 0 & \text{Otherwise} \end{cases} \tag{5}$$

$$Congestion^i_{veh}(t) = \begin{cases} e^{r \cdot \sigma^i_{veh}(t)} & \text{if} \quad \sigma^i_{veh}(t) \geq 1 \\ 0 & \text{Otherwise} \end{cases} \tag{6}$$

When the saturation degree of node $i$ is greater than 1, pedestrians or vehicles are congested with each other [39]. The higher the congestion degree is, the more serious the crowding situation is in node $i$.

The total congestion degree in node $i$ at time $t$ can be calculated by the following equation:

$$Congestion_i(t) = Congestion^i_{ped}(t) + Congestion^i_{veh}(t) \tag{7}$$

According to the pedestrian–vehicle congestion degree calculated during each time interval $\Delta t$, the cumulative pedestrian–vehicle congestion degree of all nodes during evacuation time $T$ can be calculated by the following equation:

$$F_3 = \sum_{i \in N} \sum_{t=0}^{T} Congestion_i(t) \Delta t \tag{8}$$

### 3.6. Evacuation model

To solve this pedestrian–vehicle mixed evacuation problem, usually more than one objective needs to be optimized simultaneously. Here, three major objectives, including minimal total evacuation time, minimal pedestrian–vehicle temporal–spatial conflict degree, and minimal temporal–spatial congestion degree are taken into account in the mixed evacuation process.

#### 3.6.1. Notation

The notation used in the problem formulation is introduced below:

- $i$ — an index for network nodes in $N$;
- $(i,j)$ — the arc from node $i$ to $j$;
- $k$ — an index for evacuees;
- $M$ — the total number of evacuees, including pedestrians and vehicles;
- $P_k$ — the evacuation path of the $k$th evacuee;
- $S_k$ — the initial node of the $k$th evacuee;
- $t^k_{ij}$ — the travel time of the $k$th evacuee passing edge $(i,j)$ in an emergency situation;
- $l_{ij}$ — the distance of edge $(i,j)$;
- $v^k_{ij}$ — the speed of the $k$th evacuee passing $(i,j)$;
- $v^k_{\max}$ — the maximum speed of the $k$th evacuee;
- $\Delta t$ — time interval;
- $T$ — evacuation time from the beginning to the time the last individual has reached an exit.

#### 3.6.2. Mathematical formulation

The conflict–congestion model for pedestrian–vehicle mixed evacuation is described below:

$$\min \; F_1 = \sum_{k=1}^{M} \sum^{(i,j) \in P_k} t^k_{ij} \tag{9}$$

$$\min \; F_2 = \sum_{i \in N} \sum_{t=0}^{T} Conflict_i(t) \cdot \Delta t \tag{10}$$

$$\min \; F_3 = \sum_{i \in N} \sum_{t=0}^{T} Congestion_i(t) \cdot \Delta t \tag{11}$$

subject to

$$t^k_{ij} = \frac{l_{ij}}{v^k_{ij}} \tag{12}$$

$$\Delta t = 20 \text{ s} \tag{13}$$

$$v^k_{ij} = \begin{cases} v^k_{\max} \cdot \exp(-\sigma^i_{ped}(t)) & \text{if} \quad k \in \text{pedestrians} \\ v^k_{\max} \cdot \exp(-\sigma^i_{veh}(t)) & \text{if} \quad k \in \text{vehicles} \end{cases} \tag{14}$$

$$v^k_{\max} = \begin{cases} 1.44 \; m/s & \text{if} \quad k \in \text{pedestrians} \\ 15 \; m/s & \text{if} \quad k \in \text{vehicles} \end{cases} \tag{15}$$

The objective $F_1$ (Eq. (9)) is to minimize total evacuation time. Eqs. (10) and (11) describe the minimization of total temporal–spatial conflict degree and total temporal–spatial congestion degree, respectively. Eq. (12) defines a function to calculate the time of the $k$th evacuee passing the edge $(i,j)$ in an emergency situation. Eq. (14) defines the traveling speed of evacuees, and the speed is decreasing with the increase of the saturation of evacuees. Eq. (15) gives the max speed for pedestrians and vehicles under emergency situation. The maximum value of speed for pedestrians was given by [40], and that for vehicles was taken from the work of Edara et al. [41].

The model presented above considers not only the individual movements of evacuees, but also the social interactions such as temporal–spatial conflict between pedestrians and vehicles and temporal–spatial congestion among evacuees, which is more realistic for pedestrian–vehicle mixed evacuation problem.

## 4. DPSONLF algorithm for mixed evacuation

Particle swarm optimization (PSO) is an evolutionary computation technique that was first developed by Kennedy and Eberhart [42]. Their original idea was to simulate the social behavior of a flock of birds trying to reach an unknown destination, such as the location of food resources, when flying through a field (search space). In PSO, each problem solution is a bird in the flock and is referred to as a “particle”. The movement of every individual is based on the leader (the one with the best performance) and on his own knowledge. In general, a model inspired by PSO assumes that the behavior of every particle is a compromise between its individual memory and a collective memory.

During emergency evacuation, the queuing behavior, self-organization, crowd psychology and sub-group phenomena of evacuees are similar to the social behavior of a swarm in nature. This kind of swarm can simulate physical system and social system. Therefore, particle swarm optimization algorithm inspired by swarms in nature is suitable for complicated system simulation and solving evacuation problem.

For the problem considered here, each person or vehicle fleeing from a public space can be considered as a particle, and the destination would represent any of the exits from the confined space under study. Initially, a number of particles are generated and distributed randomly around the study area. Different kinds of particles can be generated, exhibiting different physical attributes. Then particles evolve in terms of their individual and social behaviors and mutually coordinate their movements towards their destinations.

The PSO algorithm has shown its robustness and efficacy in solving function-value optimization problems in real-number space [43,44]. A modification of the PSO algorithm for solving problems with binary-valued solution elements has been developed by the initiators of PSO [45].

To facilitate the conversion from continuous real numbers to discrete-valued space, it is necessary to redefine the position and velocity of a particle and the fundamental operations which are crucial to develop a discrete particle swarm optimization algorithm.

### 4.1. Fundamental operations of DPSO

Let $X$ and $V$ be the position vector and velocity vector of any particle. $X$ can be defined as $X=(x_1,x_2,...,x_i,...,x_N)$, $1 \le i \le N$, $1 \le x_i \le N$, and $V$ is represented as $v=(v_1,v_2,...,v_i,...,v_N)$, $1 \le i \le N$, $1 \le v_i \le N$, with a binary value of 1 or 0 for each $v_i$. The fundamental operations [46] of DPSO are described in detail as follows.

1. *Subtraction operation*: a new velocity is calculated by the subtraction of two positions, as defined in the following:

$$V = X_2 - X_1 \tag{16}$$

Differences between the current position $X_1$ and a desired position $X_2$ can be presented by an array of $n$ elements in which each element represents whether or not the content of the corresponding element in $X_1$ is different from the desired state. If yes, that element gets its value from $X_2$; otherwise, the value for the element is 0. Eq. (17) illustrates the manner in which the subtraction operator is applied:

$$\begin{cases} 0 & \text{if} \quad x_{1,i} = x_{2,i} \\ x_{2,i} & \text{Otherwise} \end{cases} \tag{17}$$

2. *Multiplication operation*: the multiplication operation for velocity in DPSO is defined as in the following equation:

$$V_2 = c \cdot V_1 \quad c \in [0,1] \tag{18}$$

where $c$ is a constant. For each element $V_{1,i}$ of $V_1$, a random value *rand* is generated; if *rand* is greater than or equal to $c$, the corresponding element $V_{2,i}$ in $V_2$ is equal to $V_{1,i}$, otherwise, it is set to 0. Any element in $V_2$ can be represented by the following equation:

$$v_{2,i} = \begin{cases} v_{1,i} & \text{if} \ \ rand \ge c \\ 0 & \text{Otherwise} \end{cases} \tag{19}$$

3. *Addition operation for velocities*: the addition operation on two velocities $V_1$ and $V_2$ to obtain a new velocity is defined by the following equation:

$$V = V_1 + V_2 \tag{20}$$

Each element of the new velocity is represented as follows:

$$v_i = \begin{cases} v_{2,i} & \text{if} \ \ rand > 0.5 \\ v_{1,i} & \text{Otherwise} \end{cases} \tag{21}$$

where *rand* is a random value which ranges from 0 to 1. Generally, $V_1+V_2 \ne V_2+V_1$.

4. *Addition operation for position and velocity*: a particle can move from the current position to the next position using its new velocity. The new position is evaluated as $X=X+V$. The formula for position update is defined in the following equation:

$$x_i = \begin{cases} x_i & \text{if} \ \ v_i = 0 \\ v_i & \text{Otherwise} \end{cases} \tag{22}$$

where $x_i$ and $v_i$ are the position and velocity of the $i$th element, respectively.

### 4.2. DPSO with neighborhood learning-factor algorithm

#### 4.2.1. Fitness function

For an evacuation routing problem, many different fitness functions could be used to evaluate particles. In this paper, the fitness value of each particle is calculated by Eq. (23), which measures the minimum distance from a particle's position to each exit

$$f(particle_i) = \min\{d_i^{exit_1}, d_i^{exit_2}, ..., d_i^{exit_m}\} \tag{23}$$

where $particle_i$ represents the $i$th particle, and $d_i^{exit_m}$ is the distance from particle $i$ to exit $m$. Eq. (23) simulates the desire of approaching to exit for evacuees.

#### 4.2.2. Movement function

In the DPSO scheme, each particle can move from its current position to a new position with its new velocity. The velocity update function is defined as follows:

$$V(t+1) = w \times V(t) + c_1 \cdot r_1(P_{pbest} - X(t)) + c_2 \cdot r_2(P_{gbest} - X(t)) \tag{24}$$

where $w$ is called the inertial weight, $c_1$ and $c_2$ are learning factors, $r_1$ and $r_2$ are random numbers between 0 and 1, $P_{pbest}$ is the best position of the particle so far, and $P_{gbest}$ is the global best position of all particles.

Each particle can move to a new position after each generation of calculations according to the two parts of Eq. (24). The first part is the *Cognition-Only* part, which operates to move a particle to its local best position through past experience gained by a learning factor $c_1$ and a difference vector between the particle's current position $X$ and its local best position $P_{pbest}$. The second, *Social-Only* part operates to move a particle to the global best position by calculating a difference vector between the particle's current position $X$ and the global best position $P_{gbest}$, where the learning factor $c_2$ is used to accelerate the movement of the particle. The velocity of the particle is modified to move it both towards its personal best position and the global best position.

Note that, according to the description above, the standard DPSO uses only *Cognition-Only* and *Social-Only* to decide the next position of each particle, which, nevertheless may easily lead to congestion for a multi-exit evacuation problem. The position of each individual is different; if all individuals learn from the same group experience (global best), individuals may crowd and congest together in some certain positions.

To improve the effectiveness of the DPSO algorithm, a neighborhood learning factor is introduced to guide the particle update velocity, not only according to the individual best position and the global best position, but also the local best position of particles in adjacent positions. This local learning mechanism avoids the phenomenon that many particles congest in certain nodes as a result of learning from the global best particle.

By this mechanism, the orientation of an individual during evacuation process is affected by four parts. The first part is the attraction of the nearest exit, which stands for the desire of an evacuee for quick evacuation. The second part is the individual's own best experience. The third part is experience from the local

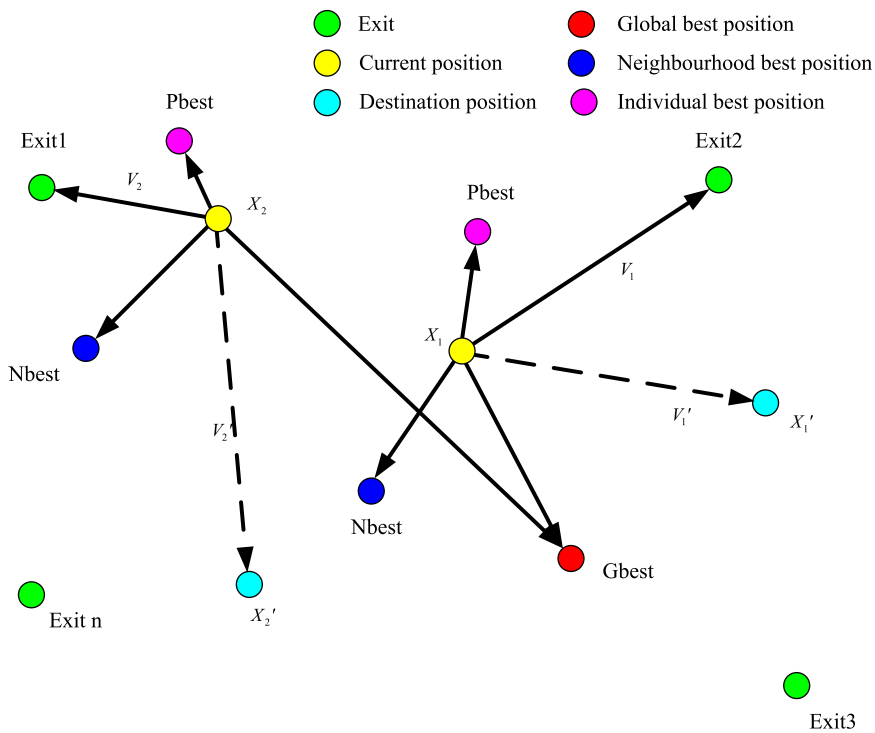


**Fig. 3.** Particle movement with self, social and neighborhood learning.

best individual in neighborhood, and the last part is learned from the global best individual. The final orientation of each evacuee synthetically depends on the four aspects. The movements of two particles are illustrated in Fig. 3. At time $t$, $X_1, X_2$ are the positions of two particles and the velocities are set towards their nearest exits, respectively. The positions of the particles at time $t+1$ are updated to new positions $X_1', X_2'$ by the mechanism consisting of self, social and neighborhood learning.

Based on the discussion above, the velocity update function can be improved as in Eq. (25), and the position update function is then represented as in Eq. (26):

$$V(t+1) = w \times V(t) + c_1 \cdot r_1(P_{pbest} - X(t)) + c_2 \cdot r_2(P_{nbest} - X(t)) + c_3 \cdot r_3(P_{gbest} - X(t)) \quad (25)$$

$$X(t+1) = X(t) + V(t+1) \quad (26)$$

where $c_1$ is a cognition factor, $c_2$ is a learning factor to accelerate the movement of the particle towards the best particle in the neighborhood, and $c_3$ is a global learning factor, $r_1$, $r_2$, and $r_3$ are random numbers between 0 and 1, and $P_{nbest}$ is the best position of a particle in the neighborhood of the particle.

In this new strategy of position updating, each individual not only considers the nearest exit but also learns from the behaviors of adjacent individuals as well as the best individual with the same individual type. Thus, the distribution of pedestrians and vehicles is more rational and the conflict can be avoided to some extent.

### 4.3. Proposed algorithm

The proposed model and DPSONLF algorithm are discrete due to the discrete nature of evacuation network. The time complexity of DPSONLF algorithm is $O(Mn^2)$, where $M$ is the number of particles and $n$ is the scale of the pedestrian–vehicle mixed evacuation problem (Fig. 4).

The DSPNLF algorithm can be described as Fig.4.

**Input:** Total number of evacuees $M$, cognition factor $c_1$, neighborhood learning factor $c_2$ and global learning factor $c_3$
**Output:** Objective values
Evacuation routes
Degree of temporal-spatial congestion and conflict

```
Randomly generate velocity and position for each particle
Initialize the status of each particle
Set the number of evacuees that are not evacuated num = M
while num > 0
  i = 1
  while i ≤ num
    Calculate the fitness value of particle i according to Eq. (23)
    Update velocity and position of particle i by Eqs. (25) and (26)
    Calculate temporal-spatial congestion and temporal-spatial conflict
    if particle i has reached any one of the exit nodes
      Mark the status of particle i as successful
      num = num − 1
    else
      Update the individual best position the neighborhood best position
      of particle i, and the global best position
    end
    i = i + 1
  end
end
```

**Fig. 4.** The DPSONLF algorithm.

## 5. Simulations and results

### 5.1. Simulation design

The area around the stadium of Wuhan Sports Center (China) was selected as the study area. This stadium contains 157 nodes, including bleachers, stairs, exits, and passages distributed over three floors, and the area outside the stadium contains 319 roads, as shown in Fig. 5. Assume that there are 5000 pedestrians inside the stadium and 5000 pedestrians outside as well. Therefore, there are 10,000 pedestrians in total in the study area. The rate of vehicle ownership in Wuhan is 93.7 cars/thousand people, according to the 2009 Annual Report of the Wuhan City Traffic Development Agency. This means that the number of vehicles in the area is 937. Simulations were carried out to simulate an evacuation process for 10,000 pedestrians and 1000 vehicles.

For the evacuation model based on temporal–spatial conflict and congestion, four approaches based on swarm intelligence: ant colony optimization (ACO) [47], multi-ant colony optimization (MACO) [17], discrete particle swarm optimization (DPSO), and discrete particle swarm optimization with neighborhood learning factor (DPSONLF) were used to simulate evacuation performance.

In this paper, 10,000 ants and 1000 ants were used to represent pedestrians and vehicles, respectively, for ACO and MACO. Correspondingly, 10,000 particles and 1000 particles were used as test data to simulate pedestrians and vehicles, respectively, in DPSO and DPSONLF. At the beginning of the simulation, 10,000 ants/particles representing pedestrians were placed randomly at the nodes of the evacuation network (5000 inside the stadium and 5000 outside), and 1000 vehicles (ants/particles) were allocated randomly at the nodes accessible to vehicles. To compare the four approaches, the initial positions of all individuals were the same for each simulation. The initial distribution of pedestrians and vehicles is shown in Fig. 6; the blue points represent pedestrians, and the red points represent vehicles. During the evacuation process under this environment integrating the stadium and the surrounding roads, the pedestrian flow evacuated from the building merges with the pedestrian flow originally existing in the roads outside, and finally this pedestrian flow mixed with the vehicle flow in the roads should evacuate to safe areas together.

The proposed DPSONLF and DPSO were implemented in a MATLAB software environment and run on a personal computer with i5-2430 M CPU and 4 GB of RAM. The updating procedures of PSO based algorithms were sequential and processed with single thread in programming. Parameters of the four methods were set as follows: $\alpha=2$, $\beta=3$, $\rho=0.7$, $Q=100$, $k=1$ for ACO [47], plus a communication coefficient $\lambda=0.5$ for MACO [17]. The inertial weights $w$, $c_1$, and $c_2$ for DPSO were set to 1, 3, and 2, respectively, and $w=1$, $c_1=3$, $c_2=3$, $c_3=2$ for DPSONLF. The parameters $c_1=3$, $c_3=2$ for DPSONLF and $c_1=3$, $c_2=2$ for DPSO were successfully used in tuning experiments following a number of suggestions [48,49].

### 5.2. Analysis of results

The proposed model was compared with other intelligent algorithms with regard to evacuation time, temporal–spatial conflict, and congestion. The sensitivity of the model and DPSONLF algorithm to learning-factor parameter setting were also discussed.

Table 1 shows the optimization results for the four approaches. Clearly the evacuation time, total time ($F_1$), cumulative degree of pedestrian–vehicle conflict ($F_2$), and degree of congestion ($F_3$) for DPSONLF are better than those for DPSO, which demonstrates that by introducing the neighborhood learning factor, on one hand, evacuation efficiency is improved, and on the other hand, conflict and congestion between pedestrians and vehicles could be effectively

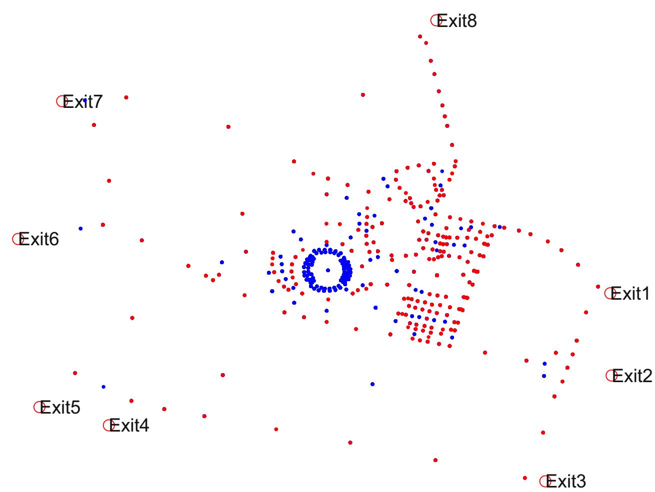


**Fig. 6.** Initial distribution of pedestrians and vehicles. (For interpretation of the references to color in this figure caption, the reader is referred to the web version of this paper.)

**Table 1**
Results of the four algorithms.

| Algorithm | $F_1$ | $F_2$ | $F_3$ | Evacuation time (s) |
|---|---|---|---|---|
| ACO | 1.0272e+007 | 21,857 | 47.57 | 22,340 |
| MACO | 1.0021e+007 | 21,487 | 44.84 | 20,680 |
| DPSO | 2.1703e+007 | 13,046 | 116.71 | 10,100 |
| DPSONLF | 2.0245e+007 | 12,021 | 68.03 | 9080 |

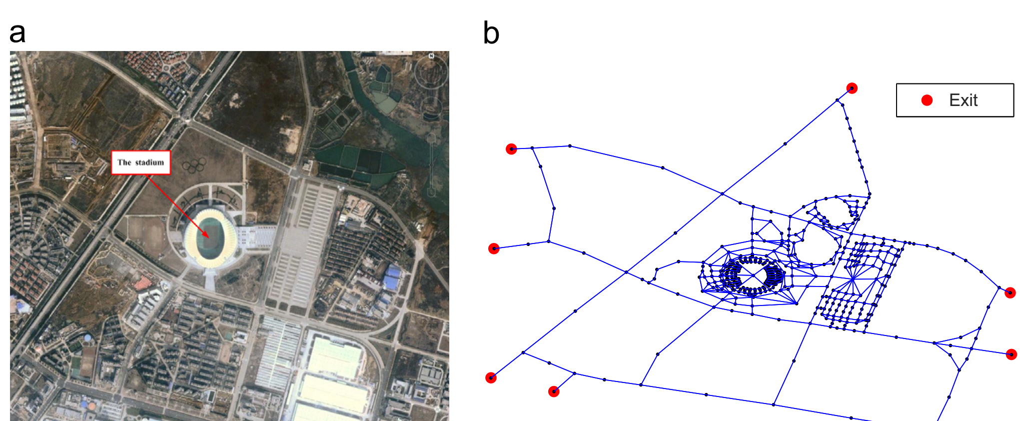


**Fig. 5.** The study area and evacuation network. (a) The study area (source: Google maps). (b) Network of the study area.

**Table 2**
Number of pedestrians at Exits 1–8.

| Algorithm | Exit 1 | Exit 2 | Exit 3 | Exit 4 | Exit 5 | Exit 6 | Exit 7 | Exit 8 | Range |
|---|---|---|---|---|---|---|---|---|---|
| ACO | 4276 | 434 | 457 | 438 | 268 | 1419 | 1393 | 1315 | 4008 |
| MACO | 4014 | 557 | 446 | 444 | 266 | 1496 | 1397 | 1380 | 3748 |
| DPSO | 43 | 59 | 166 | 3264 | 1883 | 3900 | 399 | 286 | 3857 |
| DPSONLF | 1572 | 348 | 1259 | 1543 | 1371 | 1743 | 899 | 1265 | 1395 |
| Difference from the average | | | | | | | | | Standard deviation |
| ACO | 1379 | −383 | −471 | −464 | −556 | 190 | 335 | −30 | 1316.29 |
| MACO | 1498 | −401 | −514 | −542 | −592 | 27 | 696 | −172 | 1223.77 |
| DPSO | 795 | 1780 | 40 | −402 | −588 | −550 | −607 | −468 | 1566.77 |
| DPSONLF | 322 | −902 | 9 | 293 | 121 | 493 | −351 | 15 | 444.70 |

**Table 3**
Number of vehicles at Exits 1–8.

| Algorithm | Exit 1 | Exit 2 | Exit 3 | Exit 4 | Exit 5 | Exit 6 | Exit 7 | Exit 8 | Range |
|---|---|---|---|---|---|---|---|---|---|
| ACO | 323 | 47 | 50 | 60 | 14 | 177 | 125 | 204 | 309 |
| MACO | 346 | 57 | 47 | 42 | 12 | 176 | 122 | 198 | 334 |
| DPSO | 15 | 12 | 81 | 442 | 212 | 139 | 43 | 56 | 430 |
| DPSONLF | 225 | 158 | 140 | 128 | 128 | 24 | 48 | 149 | 201 |
| Difference from the average | | | | | | | | | Standard deviation |
| ACO | 198 | −78 | −75 | −65 | −111 | 52 | 0 | 79 | 104.47 |
| MACO | 221 | −68 | −78 | −83 | −113 | 51 | −3 | 73 | 111.58 |
| DPSO | −110 | −113 | −44 | 317 | 87 | 14 | −82 | −69 | 144.69 |
| DPSONLF | 100 | 33 | 15 | 3 | 3 | −101 | −77 | 24 | 63.29 |

avoided. It can be also seen that the total evacuation time, cumulative pedestrian–vehicle conflict, cumulative degree of pedestrian–vehicle congestion, and evacuation time for MACO are smaller than those for ACO. This shows that MACO can accelerate the evacuation process and decrease pedestrian–vehicle conflict due to separate evolution of each ant colony. Temporal–spatial conflict and evacuation time for DPSONLF are the least among the four approaches. However, total evacuation time and temporal–spatial congestion of the methods based on particle swarm optimization are greater because of the learning mechanism of the particle swarm optimization algorithm.

Tables 2 and 3 list the numbers of pedestrians and vehicles evacuated from the eight exits using the four approaches. It is apparent that all eight exits are used effectively by the four algorithms. Comparing the differences from the mean value for each exit, the differences between the number of pedestrians or vehicles evacuated from each exit and the average value in ACO, MACO, and DPSO are larger than for DPSONLF.

The pedestrian/vehicle distributions of ACO, MACO, and DPSO show obviously unbalanced characteristics. Moreover, the ranges of pedestrian numbers at each exit are nearly as high as 4000 people, while the ranges of vehicle numbers are greater than 300. This means that a large number of evacuees selected a minority of exits, such as Exits 1 and 8, while the other exits were selected by only a small number of evacuees. With regard to standard deviation, DPSONLF has the minimum value among the four approaches, which indicates that DPSONLF could evacuate massive numbers of pedestrians and vehicles evenly to the eight exits, making full use of all exits.

During the process of evacuation, each individual is in one of the four states: normal, evacuating, clogging, and safe. If many evacuees are trapped in a clogging state at a certain time, this indicates that a higher degree of congestion and potential pedestrian–vehicle conflict may happen at this time. Figs. 7 and 8 depict the curves of the number of pedestrians/vehicles in a clogging state over time. The number of individuals in a clogging state according to the four algorithms is larger during the period 0–5000 s, especially before 2000 s. The greatest number of clogging evacuees is predicted by DPSO, which is in accordance with Table 1.

According to the analysis of the results shown in Figs. 7 and 8, it can be concluded that the main evacuation period is from 0 to

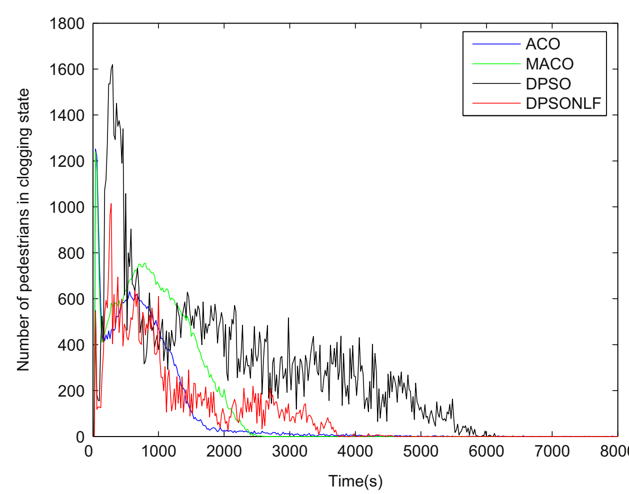


**Fig. 7.** Number of pedestrians in a clogging state at different times.

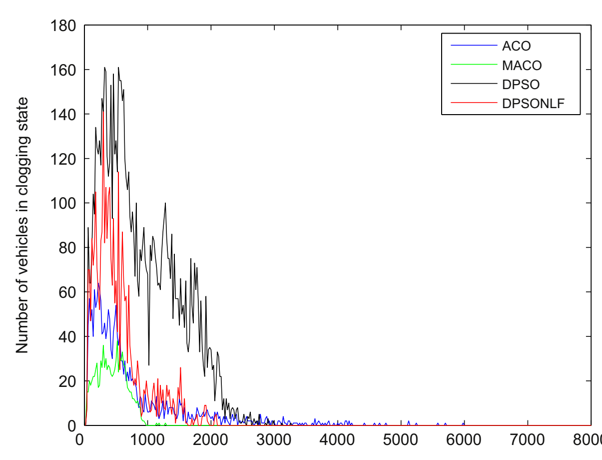


**Fig. 8.** Number of vehicles in a clogging state at different times.

2000 s. Therefore, conflict and congestion during this period will be further discussed. Fig. 9 shows time variations in conflict by different colors changing from blue to red in the legend, representing different conflict levels from low to high. There is no pedestrian–vehicle conflict inside the stadium because nodes inside the stadium are not accessible to vehicles. Pedestrian–vehicle conflict occurs mainly in the roads outside. It can be seen that pedestrian–vehicle conflict emerges in many nodes during the time period as predicted by ACO and MACO. However, pedestrian–vehicle conflict according to the PSO-based approaches is significantly reduced both in time and in space. In particular, the least pedestrian–vehicle conflict occurs in the temporal–spatial distribution predicted by DPSONLF because of the introduction of the neighborhood learning factor. Fig. 9 illustrates that the values of pedestrian–vehicle conflict predicted by DPSO and DPSONLF are smaller than those predicted by ACO and MACO. Among the four algorithms, DPSONLF predicts the minimum amount of pedestrian–vehicle conflict.

Temporal–spatial congestion by the four algorithms is shown in Fig. 10. As a result of heuristic information, evacuees in ACO and MACO are more crowded inside the stadium than evacuees in

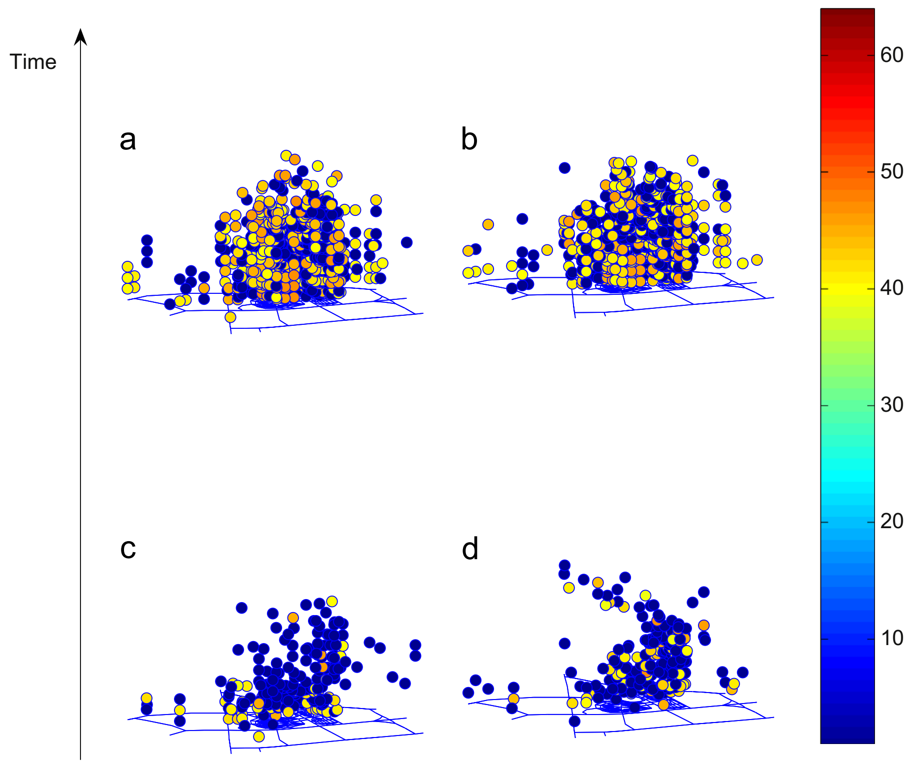


**Fig. 9.** Pedestrian–vehicle temporal–spatial conflict in the four algorithms. (a) ACO, (b) MACO, (c) DPSO and (d) DPSONLF. (For interpretation of the references to color in this figure caption, the reader is referred to the web version of this paper.)

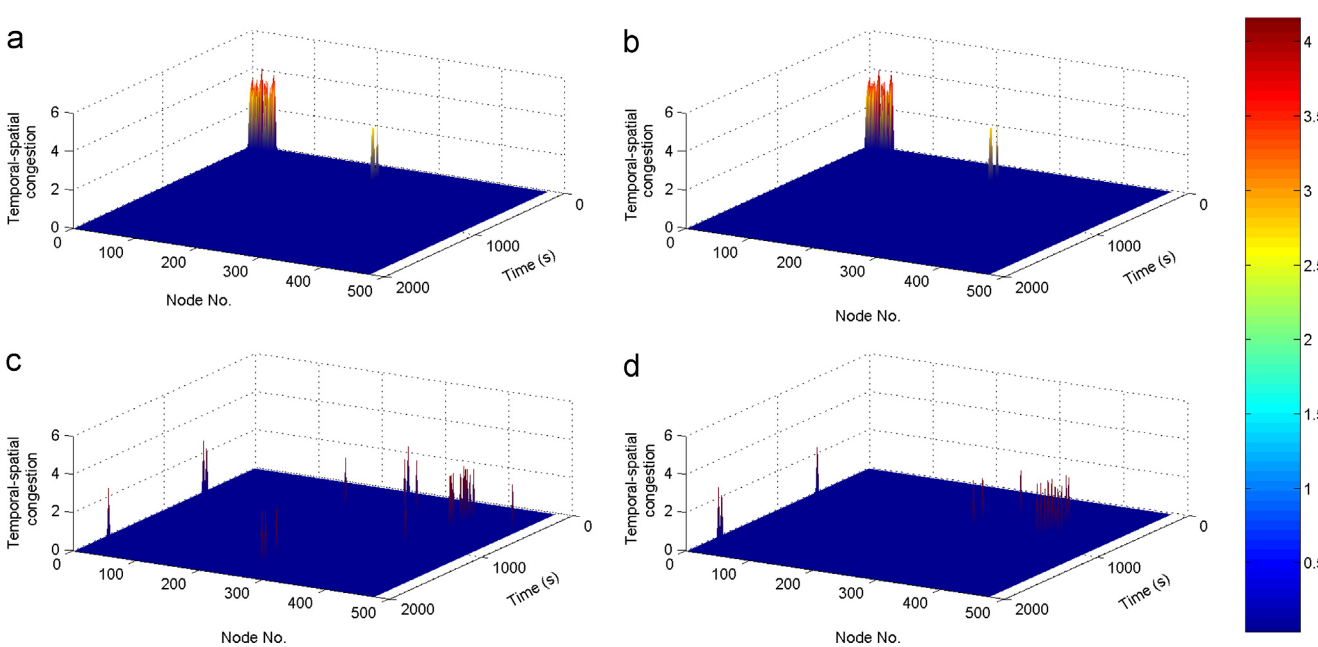


**Fig. 10.** Temporal–spatial congestion as predicted by the four algorithms.

DPSO and DPSONLF. The degree of congestion even rose to more than 3, which is rather dangerous for a large common place that accommodates a huge number of pedestrians. In contrast, the degree of congestion inside the stadium by DPSO and DPSONLF is much lower, which reduces potential safety hazards. Fig. 10 shows that the degree of congestion in DPSONLF is always maintained at a lower level both in time and in space, which shows that temporal–spatial congestion can be controlled effectively by DPSONLF.

The congestion degree increases gradually in the algorithms based on particle swarm optimization due to the learning mechanisms. Congestion occurs mainly in the interior (Nos. 1–157), outside in the road network (Nos. 250–300, 350–400), and at the exit nodes. Therefore, traffic flow in those nodes should be monitored and directed effectively and emphatically to avoid serious congestion.

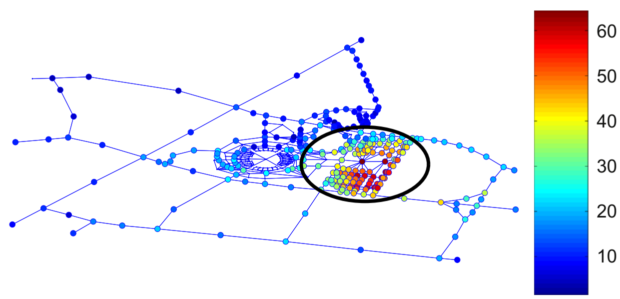


**Fig. 11.** Pedestrian–vehicle conflict levels. (For interpretation of the references to color in this figure legend, the reader is referred to the web version of this article).

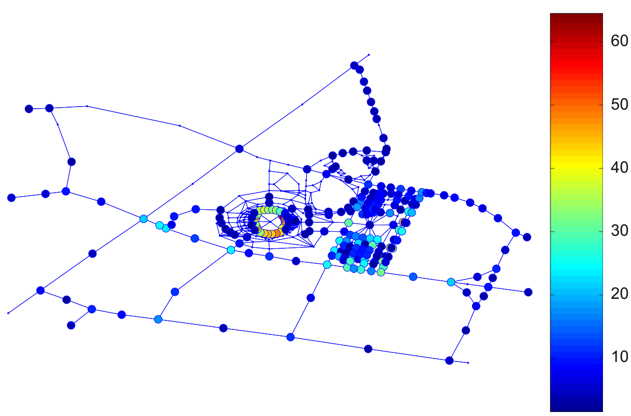


**Fig. 12.** Levels of congestion.

Fig. 11 shows the conflict level at each node in the evacuation network by DPSONLF. The node color varies from blue to red, which indicates whether the conflict level at the node is low or high. The results show that there is little conflict inside the stadium and that pedestrian–vehicle conflict occurs mainly in the outside area. Pedestrian–vehicle conflict becomes especially serious in the marked areas because of the complexity of the roads in these areas. Effective measures should be taken to guide pedestrians and vehicles and to prevent secondary conflicts.

The level of congestion during the evacuation process is shown in Fig. 12. Most of the roads are not very crowded except in several areas, especially inside the stadium, because at the beginning of the evacuation, pedestrians gather and crowd together toward the outer area inside the stadium. As the pedestrian flow gradually disperses into the outside road network, the overall extent of congestion becomes uniform. Therefore, decision-makers can plan reasonable evacuation strategies, attaching special importance to initial conditions to prevent accidents such as crowding or stampedes in enclosed spaces with massive numbers of people.

Different initial scenarios, including all the pedestrians are located in the stadium, all the pedestrians are in the road network outside, and pedestrians distribute inside and outside the stadium were considered to assess the effectiveness of the proposed approach as listed in Table 4. $P_{inside}$ and $P_{outside}$ represent the number of pedestrians inside and outside the stadium, respectively. It can be found that the values of $F_1$ and $F_3$ are larger when all the pedestrians are placed inside the stadium at beginning because so many pedestrians congested in a confined space. When all pedestrians are initially located outside the stadium, the cumulative degree of pedestrian–vehicle conflict ($F_2$) is higher due to the interaction between pedestrians and vehicles, while evacuation time is shorter since there is no need to evacuate people from the stadium. Thus, it is necessary to decrease the number of pedestrians in the stadium as far as possible or evacuate people from the stadium as soon as possible. With the increase of both pedestrians and vehicles in the whole area, the cumulative degree of temporal–spatial congestion and evacuation time by the methods based on ACO increase dramatically while those gained from approaches based on PSO do not change so obviously and the evacuation time is reduced significantly, which further shows the efficiency of PSO-based methods.

Various experiments were conducted to test the sensitivity of the proposed model to neighborhood learning-factor parameter settings. Table 5 lists the evacuation performances under different values of the neighborhood learning factor. With increasing neighborhood learning factor, the cumulative degree of pedestrian–vehicle conflict

**Table 4**
Results of different initial distributions.

| Algorithm | $P_{inside}$ | $P_{outside}$ | Vehicle | $F_1$ | $F_2$ | $F_3$ | Evacuation time (s) |
|---|---|---|---|---|---|---|---|
| ACO | 5000 | 5000 | 1000 | 1.0272e+007 | 21,857 | 47.57 | 22,340 |
| | 10,000 | 0 | 1000 | 1.1344e+007 | 12,184 | 411.1 | 74,600 |
| | 0 | 10,000 | 1000 | 1.0234e+007 | 27,905 | 172.96 | 21,920 |
| | 10,000 | 10,000 | 2000 | 2.2379e+007 | 33,272 | 834.98 | 65,240 |
| MACO | 5000 | 5000 | 1000 | 1.0021e+007 | 21,487 | 44.84 | 20,680 |
| | 10,000 | 0 | 1000 | 1.1007e+007 | 11,380 | 404.79 | 45,680 |
| | 0 | 10,000 | 1000 | 9.7928e+006 | 26,608 | 166.7 | 16,560 |
| | 10,000 | 10,000 | 2000 | 2.1486e+007 | 31,123 | 748.72 | 56,920 |
| DPSO | 5000 | 5000 | 1000 | 2.1703e+007 | 13,046 | 116.71 | 10,100 |
| | 10,000 | 0 | 1000 | 2.5852e+007 | 14,640 | 300.71 | 9560 |
| | 0 | 10,000 | 1000 | 2.0207e+007 | 23,272 | 185.62 | 18,960 |
| | 10,000 | 10,000 | 2000 | 5.1154e+007 | 26,749 | 917.74 | 16,700 |
| DPSONLF | 5000 | 5000 | 1000 | 2.0245e+007 | 12,021 | 68.03 | 9080 |
| | 10,000 | 0 | 1000 | 2.3451e+007 | 13,890 | 294.65 | 9140 |
| | 0 | 10,000 | 1000 | 1.8067e+007 | 11,927 | 177.69 | 8260 |
| | 10,000 | 10,000 | 2000 | 4.8764e+007 | 22,766 | 651.19 | 10,380 |

($F_2$) decreases, while the degree of congestion ($F_3$) increases, and the evacuation time shows a downward trend. Larger values of the neighborhood learning factor mean that each individual would like to learn more from the experience of surrounding individuals. A pedestrian or vehicle follows the evacuation route of the best pedestrian or vehicle in its neighborhood. Therefore, conflict between pedestrians and vehicles decreases, and the whole evacuation process is accelerated. Relying more on the best individual in a neighborhood, however, results in clumping of evacuees, this in turn causes congestion. Therefore, the value of the neighborhood learning factor should be set appropriately according to various considerations, which offers decision support for plan makers to achieve different performances based on different requirements. Here, a neighborhood learning factor $c_2=3$ was used to obtain better performance.

The influence of the three learning factors $c_1$, $c_2$, $c_3$ on evacuation effects, including $F_1$, $F_2$, $F_3$ and evacuation time, is shown in Fig. 13. $c_1$, $c_2$, $c_3$ vary from 0 to 3, and the corresponding point, whose color changes from blue to red and size varies from large to small, represents the values of $F_1$, $F_2$, $F_3$ and evacuation time change from small to large. It can be seen that $F_1$ and evacuation time are better when $c_1$, $c_2$, $c_3$ are set to smaller values. $F_2$ and $F_3$ are smaller with larger $c_1$, $c_2$ and smaller $c_3$.

Fig. 14 draws the number of non-dominated solutions with different generations of the DPSONLF algorithm. It illustrates that with the increase of generations, the number of non-dominated solutions becomes larger and a relatively stable number of non-dominated solutions are achieved after 150 generations. In this study, 15 non-dominated solutions are obtained by repeating the implementation 10 times.

**Table 5**
Results of different neighborhood learning factors.

| $c_2$ | $F_1$ | $F_2$ | $F_3$ | Evacuation time (s) |
|---|---|---|---|---|
| 1 | 2.5383e+007 | 16,280 | 49.18 | 13,700 |
| 2 | 2.3418e+007 | 15,887 | 54.55 | 13,340 |
| 3 | 2.0245e+007 | 12,021 | 68.03 | 9080 |
| 4 | 1.9456e+007 | 10,516 | 130.51 | 7480 |
| 5 | 1.9382e+007 | 8932.1 | 144.61 | 7720 |

## 6. Conclusions

By studying the particular phenomena of individuals during emergency evacuations, including crowd psychology, sub-group phenomena, and other aspects, swarm intelligence theory has been used in this research to simulate and optimize a mixed pedestrian–vehicle evacuation process. Pedestrian–vehicle temporal–spatial conflict and temporal–spatial congestion are defined. An evacuation model based on minimizing evacuation time, temporal–spatial conflict, and congestion is presented. A DPSONLF algorithm is proposed to solve the mixed pedestrian–vehicle evacuation problem. In this approach, each evacuated individual is considered as a particle. The particles move in terms of their own experience and that of the best individual in the swarm; in addition, they learn from the best particle in their respective neighborhoods. This mechanism integrates individual, local, and global learning and simulates the individual's behavior of going with the crowd as well as accelerating the process of searching for exits. The simulation results of the ant colony optimization algorithm, multi-ant colony optimization algorithm, particle swarm optimization algorithm, and DPSONLF algorithm were compared and analyzed. The results indicate that DPSONLF has better performance in the control of

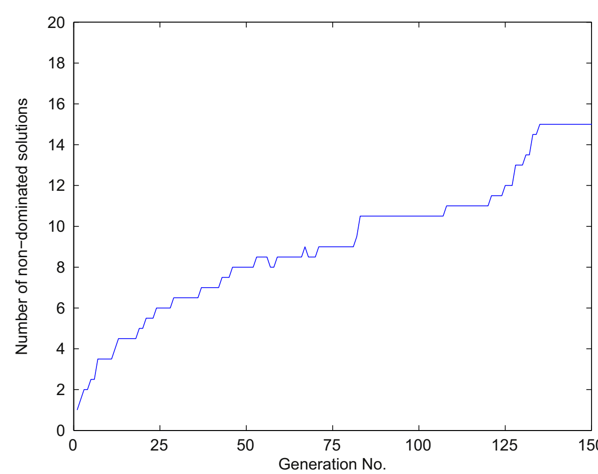


**Fig. 14.** Number of non-dominated solutions in generations.

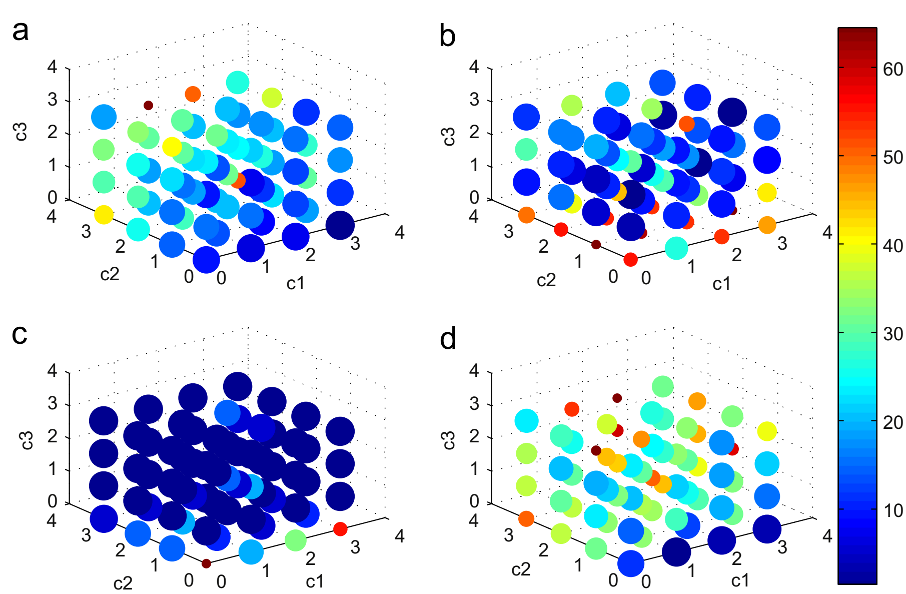


**Fig. 13.** Performances with different $c_1$, $c_2$ and $c_3$. (a) F1, (b) F2, (c) F3 and (d) Evacuation Time.

conflict and congestion both in time and in space during the evacuation process for mixed pedestrians and vehicles.

The simulation results show that the methods based on particle swarm optimization have better performance with regard to pedestrian–vehicle temporal–spatial conflict and evacuation time than the methods based on the ant colony optimization algorithm. However, the total evacuation time and the degree of temporal–spatial congestion predicted by the particle swarm optimization methods are greater. By analyzing the number of pedestrians/vehicles evacuated from each exit, pedestrian–vehicle temporal–spatial conflict, and temporal–spatial congestion, it has been demonstrated that the DPSONLF algorithm can evacuate pedestrians and vehicles from each exit more evenly than other algorithms while maintaining a lower rate of conflict.

Future research will involve improvement of the DPSONLF algorithm to decrease congestion, because particles follow the best particle in the group by the learning mechanism of the particle swarm optimization algorithm. Another challenging subject for future research is to applying the model to massive evacuation simulation and improving the computational efficiency.

## Acknowledgments

This work was supported in part by the National Science Foundation of China (Grants #61202287, #61170202, #40971233), partly sponsored by the National Science Foundation of China (Grants #61170135), Wuhan Municipal Key Scientific and Technological Projects Funding (Grant #201210121029). The authors would also like to thank the anonymous reviewers for their valuable comments and suggestions.

## References

[1] Liu Y, Fan ZP, Zhang Y. Risk decision analysis in emergency response: a method based on cumulative prospect theory. Comput Oper Research 2014;42:75–82.
[2] Liu X, Li W, Tu YL, Zhang WJ. An expert system for an emergency response management in Networked Safe Service Systems. Exp Syst Appl 2012;39:8300–11.
[3] Ma J, Song WG, Tian W, Lo SM, Liao GX. Experimental study on an ultra high-rise building evacuation in China. Safety Sci 2012;50:1665–74.
[4] Bretschneider S, Kimms A. A basic mathematical model for evacuation problems in urban areas. Transp Res Part A 2011;45:523–39.
[5] Si B, Zhong M, Gao Z. Link resistance function of urban mixed traffic network. J Transp Syst Eng Inf Technol 2008;8(1):68–73.
[6] Xie DF, Gao ZY, Zhao XM, Li KP. Characteristics of mixed traffic flow with non-motorized vehicles and motorized vehicles at an unsignalized intersection. Physica A 2009;388(10):2041–50.
[7] Li Q, Wang B. Properties of vehicle gap distribution in the mixed traffic flow. Proc Eng 2012;31:1001–5.
[8] Hu X, Wang W, Yang H. Mixed traffic flow model considering illegal lane-changing behavior: simulations in the framework of Kerner's three-phase theory. Phys A: Stat Mech Appl 2012;391(21):5102–11.
[9] Meng J, Dai S, Dong L, Zhang J. Cellular automaton model for mixed traffic flow with motorcycles. Physica A 2007;380:470–80.
[10] Koo J, Kim YS, Kim B, Christensen KM. A comparative study of evacuation strategies for people with disabilities in high-rise building evacuation. Exp Syst Appl 2013;40:408–17.
[11] Li J, Zhang B, Liu W, Tan Z. Research on OREMS-based large-scale emergency evacuation using vehicles. Process Safety Environ Protect 2011;89:300–9.
[12] Chen CK, Li J, Zhang D. Study on evacuation behaviors at a T-shaped intersection by a force-driving cellular automata model. Physica A 2012;391:2408–20.
[13] Guo RY, Huang HJ, Wong SC. Route choice in pedestrian evacuation under conditions of good and zero visibility: experimental and simulation results. Transp Res Part B 2012;46:669–86.
[14] Tanaka K, Nagatani T, Hanaura H. Traffic mixing in deterministic two-lane model of Hurricane evacuation. Physica A 2007;380:490–502.
[15] Bretschneider S, Kimms A. Pattern-based evacuation planning for urban areas. Eur J Oper Res 2012;216:57–69.
[16] Jin M, Chen T, Shen S. Influence of transport mode choice on evacuation time in mixed traffic flow evacuation simulations. J Tsinghua Univ (Sci Technol) 2009;49(2):179–82.
[17] Zong XL, Xiong SW, Fang ZX, Li QP Multi-ant colony system for evacuation routing problem with mixed traffic flow. In: Proceedings of the 2010 IEEE congress on evolutionary computation; 2010. p. 1–6.
[18] Liu L, Mu H, Luo H, Li X. A simulated annealing for multi-criteria network path problems. Comput Oper Res 2012;39:3119–35.
[19] Liberatore F, Ortuño MT, Tirado G, Vitoriano B, Scaparra MP. A hierarchical compromise model for the joint optimization of recovery operations and distribution of emergency goods in Humanitarian Logistics. Comput Oper Res 2014;42:3–13.
[20] Yang B, Ren B, Wu YG. The research of multi-resolution modeling and simulation of the emergency evacuation. Proc Eng 2012;29:3110–6.
[21] Mei Z, Dong W, Pan G, Zhang P, Zhang Y. Adaptive ant colony algorithm based on evacuation wayfinding optimization model in building fire. J Shenyang Jianzhu Univ (Nat Sci) 2008;24(4):671–4.
[22] Yuan Y, Wang D. Path selection model and algorithm for emergency logistics management. Comput Ind Eng 2009;56:1081–94.
[23] Izquierdo J, Montalvo I, Pérez R, Fuertes VS. Forecasting pedestrian evacuation times by using swarm intelligence. Physica A 2009;388(7):1213–20.
[24] Zheng Y, Chen J, Wei J, Guo X. Modeling of pedestrian evacuation based on the particle swarm optimization algorithm. Phys A: Stat Mech Appl 2012;391(17):4225–33.
[25] Zheng XP, Cheng Y. Conflict game in evacuation process: a study combining cellular automata model. Physica A 2011;390:1042–50.
[26] Chooramun N, Lawrence PJ, Galea ER. An agent based evacuation model utilising hybrid space discretisation. Safety Sci 2012;50(8):1685–94.
[27] Manley M, Kim YS. Modeling emergency evacuation of individuals with disabilities (exitus): an agent-based public decision support system. Exp Syst Appl 2012;39(9):8300–11.
[28] Saadatseresht M, Mansourian A, Taleai M. Evacuation planning using multiobjective evolutionary optimization approach. Eur J Oper Res 2009;198(1):305–14.
[29] Liao Z, Mao X, Hannam PM, Zhao T. Adaptation methodology of CBR for environmental emergency preparedness system based on an Improved Genetic Algorithm. Exp Syst Appl 2012;39:7029–40.
[30] Xie C, Turnquist MA. Lane-based evacuation network optimization: an integrated Lagrangian relaxation and tabu search approach. Transp Res Part C 2011;19:40–63.
[31] Stepanov A, Smith JM. Multi-objective evacuation routing in transportation networks. Eur J Oper Res 2009;198(2):435–46.
[32] Tzeng GH, Cheng HJ, Huang TD. Multi-objective optimal planning for designing relief delivery systems. Transp Res Part E 2007;43:673–86.
[33] Lim GJ, Zangeneh S, Baharnemati MR, Assavapokee T. A capacitated network flow optimization approach for short notice evacuation planning. Eur J Oper Res 2012;223:234–45.
[34] Fang ZX, Li QP, Qingquan Li QQ, Han LD, Shaw SL. A space–time efficiency model for optimizing intra-intersection vehicle–pedestrian evacuation movements. Transp Res Part C 2013;31:112–30.
[35] Pires TT. An approach for modeling human cognitive behavior in evacuation models. Fire Safety J 2005;40(2):177–89.
[36] Lee D, Park J, Kim H. A study on experiment of human behavior for evacuation simulation. Ocean Eng 2004;31(8-9):931–41.
[37] Levinson HS, Potts IB, Harwood DW, Gluck J, Torbic DJ. Safety of U-turns at unsignalized median openings: some research findings. Transp Res Rec: J Transp Res Board 2005;1912:72–81.
[38] Zong XL, Xiong SW, Fang ZX. Optimization and proportion analysis of pedestrian–vehicle mixed evacuation based on ant colony algorithm. Syst Eng: Theor Pract 2012;32(7):1610–7.
[39] Chen Y, Xiao D. Traffic network flow forecasting under congested situation. Chin J Sci Instr 2008;29(8):111–6.
[40] Moussaid M, Helbing D, Garnier S, Johansson A, Combe M, Theraulaz G Experimental study of the behavioural mechanisms underlying self-organization in human crowds. Proc R Soc B: Biol Sci 2009;276:2755–62.
[41] Edara P, Sharma S, McGhee C. Development of a large-scale traffic simulation model for hurricane evacuation: methodology and lessons learned. ASCE Nat Hazards Rev 2010;11(4):127–39.
[42] Kennedy J, Eberhart RC. Particle swarm optimization. In: Proceedings of the 1995 IEEE international conference on neural network; 1995. p. 1942–8.
[43] Shigenori N, Takamu G, Toshiku Y, Yoshikazu F. A hybrid particle swarm optimization for distribution state estimation. IEEE Trans Power Syst 2003;18:60–8.
[44] Yoshida H, Kawata K, Fukuyama Y, Nakanishi Y A particle swarm optimization for reactive power and voltage control considering voltage stability. In: Proceedings of the international conference on intelligent system application to power systems; 1999. p. 117–21.
[45] Kennedy J, Eberhard RC A discrete binary version of the particle swarm algorithm. In: Proceedings of IEEE conference on systems, man, and cybernetics; 1997. p. 4104–9.
[46] Tsai KH, Wang TI, Hsieh TC, Chiu TK, Lee MC. Dynamic computerized testlet-based test generation system by discrete PSO with partial course ontology. Exp Syst Appl 2010;37(1):774–86.
[47] Fang ZX, Zong XL, Li QQ, Li QP, Xiong SW. Hierarchical multi-objective evacuation routing in stadium using ant colony optimization approach. J Transp Geogr 2011;19(3):443–51.
[48] Liao CJ, Tseng CT, Luarn P. A discrete version of particle swarm optimization for flowshop scheduling problems. Comput Oper Res 2007;34(10):3099–111.
[49] Montalvo I, Izquierdo J, Pérez R, Tung MM. Particle swarm optimization applied to the design of water supply systems. Comput Math Appl 2008;56(3):769–76.